JOURNAL OF AIRCRAFT
Vol. 48, No. 5, September–October 2011

Engineering Notes

Extended Nonlinear Lifting-Line Method for Aerodynamic Modeling of Reconfigurable Aircraft

Adam M. Wickenheiser*
George Washington University, Washington, D.C. 20052
and
Ephrahim Garcia
Cornell University, Ithaca, New York 14853

DOI: 10.2514/1.C031406

Nomenclature

C_l	=	section lift coefficient
c	=	local chord length
D	=	fading-memory constant
G	=	nondimensional circulation
l	=	section lift force/length
m	=	number of points used in sine series expansion of circulation function
N	=	consecutive iterations convergence parameter
r	=	perpendicular distance from vortex
tol	=	iteration relative tolerance of conversion
U_∞	=	freestream velocity magnitude
w	=	downwash velocity
y_0	=	wing semispan, y coordinate of wingtip
α	=	wind incidence angle, wing angle of attack
α_{eff}	=	effective angle of attack
α_{2D}	=	2-D vortex-induced wind incidence angle
α_{3D}	=	3-D wake-induced wind incidence angle
Γ	=	circulation magnitude
η	=	nondimensional spanwise coordinate
θ	=	local wing twist angle
Λ	=	local wing sweep angle
ξ	=	nondimensional chordwise coordinate
ρ	=	air density
ϕ	=	trigonometric spanwise coordinate

I. Introduction

THE preliminary design of morphing aircraft [1–7] requires aerodynamic analyses at widely varying flight conditions and geometric configurations. Thus, a fast, adaptable algorithm is required that can accept geometric "morphing" parameter variations and recompute the wing (or aircraft) aerodynamic characteristics. Lifting-line theory, first developed by Prandtl and Tietjins [8] and Munk [9], is chosen because it fulfills these needs and is readily programmed to populate large, multidimensional lookup tables for reconfigurable aircraft simulation [7]. The basis of the lifting-line technique used in the present study is Weissinger's method for straight, swept wings [10]. This method uses a flow-tangency (i.e., impermeability) condition at the three-quarter-chord curve of the wing, which avoids the singularity Prandtl's method introduces for swept wings when the effects of bound vorticity are incorporated.

Prandtl's and, indeed, Weissinger's methods assume that the airfoil section lift curves are linear (that is, the lift coefficient at any angle of attack is fully described by the zero-lift angle of attack and the lift-curve slope) and that the section drag coefficients are identically zero, i.e., that the flow is inviscid. A common method to incorporate nonlinear sectional data is to iterate on the lifting-line formulation via a weighted averaging technique that blends the linearized potential flow over the wing with the nonlinear sectional data. This iterative procedure originates with the work of Tani [11] and Multhopp [12], who have developed a numerical integration technique similar to Gaussian quadrature for computing the net lift contribution of the spanwise circulation distribution using sine series. The coefficients of these series have been formalized and tabulated by Sivells and Neely [13]. More recently, this method has been used to calculate the aerodynamic characteristics of drooped leading-edge wings around stall [14]. It should be noted that the above studies have been restricted to straight wings so that Prandtl's formulation can be used. Owens [15] has applied this iterative technique to Weissinger's method for straight, swept wings.

Several extensions/generalizations to Weissinger's method have been developed subsequently. Wing quarter-chord curves described by polynomial equations have been analyzed using modified lifting-line theory for stationary [16] and oscillating wings [17]. Wickenheiser and Garcia [18] have generalized this formulation to wings of arbitrary, piecewise continuous curvature. Phillips and Snyder [19] have developed a technique using 3-D vortex elements that uses Newton's method to solve the resulting system of nonlinear equations.

The present study is based on modifications to the authors' previous work on curved lifting lines [18]. First, a summary of the salient features of the generalized Weissinger's method is given, followed by a presentation of the modifications to this method necessary to incorporate nonlinear section data. An iterative procedure is developed whose purpose is to cause the convergence of the results of the Weissinger's method and the results using the sectional aerodynamic data. Subsequently, the results of this technique are compared with wind-tunnel data for elliptical and crescent wings at a Reynolds number $Re = 1.7 \times 10^6$ [20] and tapered wings at $Re = 3.49 \times 10^6$ [13].

II. Method Formulation

The lifting-line technique used in this study consists of two phases. In the first phase, a modified Weissinger method for planar, curved wings is used to compute an initial guess of the circulation distribution along the span and to populate the matrix of coefficients used in the downwash calculations in the second phase. The first phase is based on the extended lifting-line technique derived in [18] and uses linearized sectional data. The second phase consists of an iterative procedure that attempts to minimize the discrepancy between the circulation distributions predicted by 1) the lifting-line analysis and 2) the Kutta–Joukowski theorem using the nonlinear sectional data, which take into account viscous effects. Brief presentations of these two phases are given in the next sections.

A. Modified Weissinger Method (Initial Phase)

As previously mentioned, this phase is based on minor modifications to the lifting-line method derived and presented in detail in [18]; thus, only the key points and equations are given herein. The Cartesian coordinate system and the layout of a typical horseshoe

Received 7 February 2011; revision received 9 May 2011; accepted for publication 10 May 2011.

*Assistant Professor, Department of Mechanical and Aerospace Engineering; amwick@gwu.edu.

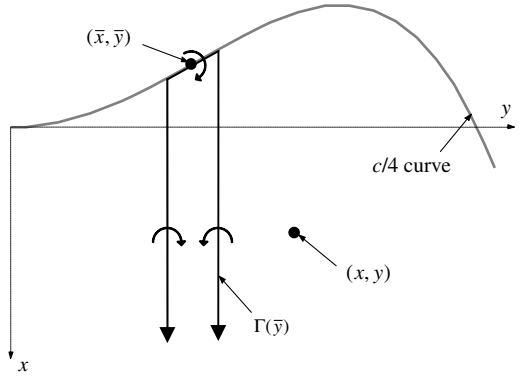

Fig. 1 Coordinate system and horseshoe-vortex structure.

vortex in the wake of the wing are shown in Fig. 1. The positive x direction points downstream, parallel to the freestream velocity U_∞, and the positive y direction points toward the right wingtip. The quarter-chord coordinates, chord length, and twist distribution are given as piecewise differentiable functions on the domain $y \in [-y_0, y_0]$. The model of the flowfield consists of a bound or lifting vortex at the quarter-chord curve of the wing and a planar trailing vortex sheet that extends to infinity downstream. The downwash at each point in the flowfield is therefore the sum of the velocities induced by the lifting vortex and the distributed vortex sheet. Since the flowfield is modeled as a superposition of potential flows, this method only applies when viscous effects are insignificant.

Assuming the flowfield structure shown in Fig. 1, the Biot-Savart Law gives the downwash at a point in the flowfield (x, y) induced by the bound and trailing vortices:

$$w(x,y) = \frac{1}{4\pi}\int_{-y_0}^{y_0} \frac{\Gamma'(\bar{y})}{y-\bar{y}}\,\mathrm{d}\bar{y} + \frac{1}{4\pi}\int_{-y_0}^{y_0} \frac{\Gamma'(\bar{y})}{y-\bar{y}} \frac{x-\bar{x}(\bar{y})}{\sqrt{(x-\bar{x}(\bar{y}))^2+(y-\bar{y})^2}}\,\mathrm{d}\bar{y} + \frac{1}{4\pi}\int_{-y_0}^{y_0} \Gamma(\bar{y}) \frac{x-\bar{x}(\bar{y})+\bar{x}'(\bar{y})(\bar{y}-y)}{[(x-\bar{x}(\bar{y}))^2+(y-\bar{y})^2]^{3/2}}\,\mathrm{d}\bar{y} \tag{1}$$

where $\Gamma'(\bar{y}) = \mathrm{d}\Gamma(\bar{y})/\mathrm{d}y$. Using the assumption that the wing's section lift-curve slope is 2π, the Pistolesi condition states that the overall wind velocity should be tangent to the plane of the wing at a perpendicular distance of one-half chord behind the bound vortex [10,21,22]. Taking into account the local sweep angle of the wing, this point is given by

$$x = \bar{x}(y) + \frac{c(y)}{2}\frac{1}{\cos\Lambda(y)} = \bar{x}(y) + \frac{c(y)}{2}\sqrt{[\bar{x}'(y)]^2+1} \tag{2}$$

At this point it is beneficial to convert Eq. (1) into nondimensional form in order to remove the scale dependency from the numerical calculations. Henceforth, the following dimensionless variables are introduced:

$$\eta = \frac{y}{y_0}, \qquad \bar{\eta} = \frac{\bar{y}}{y_0}, \qquad G = \frac{\Gamma}{y_0 U_\infty}, \qquad \bar{\xi} = \frac{\bar{x}}{c}, \qquad \alpha = \frac{w}{U_\infty} \tag{3}$$

To simplify the evaluation of the integrals in Eq. (1), the nondimensional circulation distribution $G(\bar{\eta})$ is cast as a sine series of m terms, given by [12]

$$G(\phi) = \sum_{n=1}^{m} G_n f_n(\phi) \tag{4}$$

where

$$f_n(\phi) \equiv \frac{2}{m+1}\sum_{k=1}^{m}\sin(k\phi_n)\sin(k\phi), \qquad G_n \equiv G(\phi_n)$$
$$\phi_n \equiv \frac{n\pi}{m+1}, \qquad \phi \equiv \cos^{-1}(\bar{\eta})$$

where $G_1, \ldots, G_m$ are the unknown coefficients to be computed. The number of terms in the sine series m directly affects the accuracy of the series representation of the circulation distribution $G(\phi)$, but it also indirectly determines the number of wing locations at which Eq. (1) must be evaluated, as will be demonstrated.

With these substitutions, Eq. (1) provides a formula for the downwash angle at $\phi_v \equiv \cos^{-1}(\eta)$ as a linear function of the unknowns $G_1, \ldots, G_m$. By the Pistolesi flow-tangency condition, this downwash angle is equal to the geometric angle of attack (wing angle of attack and local twist angle). Evaluating this angle at the locations $\phi_1, \ldots, \phi_m$ defined in Eq. (4) gives a square system of linear equations $\boldsymbol{\alpha} = \mathbf{AG}$, where

$$\mathbf{A_{vn}} = \frac{1}{\pi(m+1)\sin\phi_v}\sum_{k=1}^{m} k\sin(k\phi_n)\sin(k\phi_v) + \frac{1}{2\pi(m+1)}\int_0^\pi \left[-P(\phi_v,\phi)\sum_{k=1}^{m} k\sin(k\phi_n)\cos(k\phi) + \left(\frac{y_0}{c(\phi_v)}\right)^2 R(\phi_v,\phi)\sin\phi\sum_{k=1}^{m}\sin(k\phi_n)\sin(k\phi)\right]\mathrm{d}\phi \tag{5}$$

[The definitions of $P(\phi_v, \phi)$ and $R(\phi_v, \phi)$ can be found in [18].] After solving this system for the unknowns $G_1, \ldots, G_m$, the circulation distribution along the wing span $G(y)$ can be reconstructed using Eq. (4).

B. Iterative Process

To incorporate nonlinear sectional aerodynamics, the Pistolesi condition, which assumes a linear sectional lift curve with slope 2π, must be relaxed. On the other hand, the iterative method should reduce to the method described in Sec. II.A if a linear section lift curve with slope 2π is assumed. To construct a consistent iterative method, first the induced velocity angle of a 2-D point vortex is defined by

$$\alpha_{2\mathrm{D}}(y) = \frac{\Gamma(y)}{2\pi U_\infty r(y)} = \frac{y_0 G(y)}{2\pi r(y)} \tag{6}$$

where $r(y)$ is the distance from the vortex. The Pistolesi condition states that, under the assumption of a linear section lift curve with slope of 2π, if $r(y) = c(y)/2$, then the effective angle of attack $\alpha_{\mathrm{eff}}(y)$ is equal to $\alpha_{2\mathrm{D}}(y)$. Thus, the flow is assumed to be tangent to the wing at this point, and so the downwash angle induced by the wake, denoted as $\alpha_{3\mathrm{D}}(y)$, is equal to the geometric angle of attack. A simple formulation of the effective angle of attack is given by

$$\alpha_{\mathrm{eff}}(y) = \alpha + \theta(y) - \alpha_{3\mathrm{D}}(y) + \alpha_{2\mathrm{D}}(y)$$

which can be seen to satisfy the Pistolesi condition under its assumptions [23].

Typically, the section lift curve is given by a generic function $C_l(\alpha_{\mathrm{eff}}(y), y)$, where the dependencies indicate that the effective angle of attack varies along the span (due to twist and downwash variations), and the lift-curve function itself varies if there is a change in airfoil along the span. These lift-curve data can be generated experimentally (as is done in this study) or computationally using a viscous solver. By the Kutta–Joukowski theorem, the circulation at each wing station is given by

$$\Gamma(y) = \frac{l(y)}{\rho U_\infty} \quad \text{or} \quad G(y) = \frac{c(y)}{2y_0} C_l(\alpha_{\mathrm{eff}}(y), y) \tag{7}$$

The circulation distribution calculated using the modified Weissinger's method in Eq. (5), which uses the assumptions of the Pistolesi condition, and the circulation distribution calculated using

Table 1 Iterative solution procedure

1) Assume $\alpha_{3D}^{(1)}(y) = \alpha + \theta(y)$ (Pistolesi condition). Thus, $\alpha_{eff}^{(1)}(y) = \alpha_{2D}^{(1)}(y)$.
2) Compute $G^{(1)}(y)$ from the modified Weissinger's method [Eq. (5)].
3) Set $n \leftarrow 1$.
4) Compute the new circulate distribution using the sectional lift and Eq. (7):

$$G_{new}(y) = \frac{c(y)}{2y_0} C_l(\alpha_{eff}^{(n)}(y), y)$$

5) If

$$\max_{y\in[-y_0,y_0]} \left| \frac{G_{new}(y) - G^{(n)}(y)}{G^{(n)}(y)} \right| < \text{tol}$$

N times consecutively, then set $G(y) \leftarrow G_{new}(y)$, $\alpha_{eff}(y) \leftarrow \alpha_{eff}^{(n)}(y)$, and quit.
6) Otherwise,

$$G^{(n+1)}(y) = (1 - D)G^{(n)}(y) + DG_{new}(y)$$

where $0 \le D \le 1$ is a fading-memory constant (or exponential smoother).
7) Compute $\alpha_{3D}^{(n+1)}(y)$ by evaluating $\boldsymbol{\alpha}_{3D}^{(n+1)} = \mathbf{A}\mathbf{G}^{(n+1)}$, where

$$\boldsymbol{\alpha}_{3D}^{(n+1)} = [\,\alpha_{3D}^{(n+1)}(\phi_1) \quad \cdots \quad \alpha_{3D}^{(n+1)}(\phi_m)\,]^T$$
$$\mathbf{G}^{(n+1)} = [\,G^{(n+1)}(\phi_1) \quad \cdots \quad G^{(n+1)}(\phi_m)\,]^T$$

8) Compute the 2-D induced velocity angle using Eq. (6):

$$\alpha_{2D}^{(n+1)}(y) = \frac{2y_0 \cos\Lambda(y)}{\pi c(y)} G^{(n+1)}(y)$$

9) Compute the induced angle of attack using

$$\alpha_{eff}^{(n+1)}(y) = \alpha + \theta(y) - \alpha_{3D}^{(n+1)}(y) + \alpha_{2D}^{(n+1)}(y)$$

10) Set $n \leftarrow n + 1$ and go to step 4.

the sectional aerodynamic data in Eq. (7) are generally not in agreement except in the theoretical situation of ideal, thin airfoils. Thus, an iterative procedure is proposed to cause these two circulation distributions to converge. The iterative process used to compute the wing circulation and effective angle of attack along the span may be summarized in Table 1, where the parenthetical superscript indicates the iteration number.

During each iteration, the circulation distribution computed from the modified Weissinger's method $G^{(n)}(y)$ is compared with the circulation distribution computed from the section aerodynamic data $G_{new}(y)$ in step 5. If, N consecutive iterations, the maximum disparity between the two is within a predefined tolerance tol, then the procedure terminates. Otherwise, the weighted average of the two is passed on to the next iteration, where the weighting D is a predetermined fading-memory constant that aids in the convergence of the two circulation distributions. A value of $D = 0.05$ has been shown to provide robust convergence for a variety of wings and so is used in this study [15]. After the iterative loop terminates, the value of $\alpha_{eff}(y)$ computed in step 5 is used to evaluate the coefficients of lift and drag at each wing station, then integrated over the span to yield the wing lift and drag coefficients.

To prove that this method is a consistent extension of the modified Weissinger method derived in Sec. II.A, consider the case in which the section lift curve is indeed linear with slope 2π. Then step 4 yields

$$G_{new}(y) = \frac{c(y)}{2y_0} 2\pi\alpha_{2D}^{(1)}(y) = \frac{\pi c(y)}{y_0} \frac{y_0 G^{(1)}(y)}{2\pi c(y)/2} = G^{(1)}(y) \quad (8)$$

which indicates that the algorithm converges on the first iteration. Consequently, steps 5–9 of the iteration also give the same results every iteration. This proves that the proposed iterative process collapses to the single-step, modified Weissinger method under ideal thin airfoil conditions.

III. Experimental Validation

To validate this computational method, results obtained from it are compared with experimental data appearing in the literature for three different wing planforms. The first comparison uses elliptical and crescent planforms from van Dam et al. [20] shown in Figs. 2a and 2b. Both of these wings are composed of a straight, rectangular inboard section and an elliptical chord distribution for the outboard section. Both wings have the same span and root chord; hence, their planform areas, aspect ratios, and mean aerodynamic chords are identical. The curvature of the quarter-chord is determined by the tip sweep distance, which indicates the position of the tip relative to the leading edge of the root. Finally, the tapered wing design from Sivells and Neely [13], depicted in Fig. 2c, is analyzed using the present method and compared with their experimental data and lifting-line

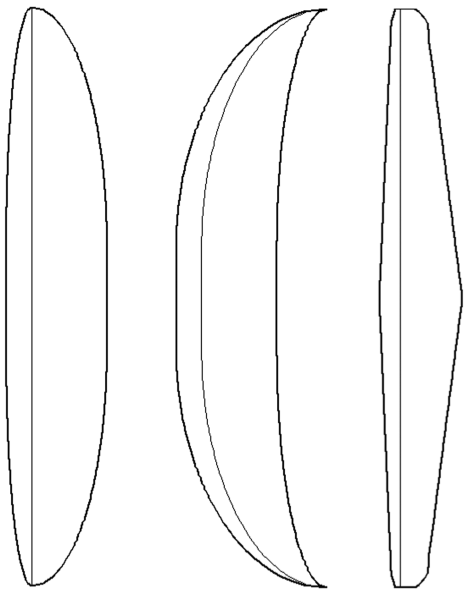

a) b) c)

Fig. 2 Planforms of three wing types: elliptical, crescent, and tapered.

Table 2 Wing geometric parameters

Parameter	Value
Elliptical wing [20]	
Wing span	6.74 ft.
Root chord	1.17 ft.
Mean aerodynamic chord	1.03 ft.
Planform area	6.47 ft^2
Aspect ratio	7.01
Reynolds number	1.7×10^6
Section shape	NACA 0012
Crescent wing [20]	
Wing span	6.74 ft.
Root chord	1.17 ft.
Tip sweep distance	1.75 ft.
Mean aerodynamic chord	1.03 ft.
Planform area	6.47 ft^2
Aspect ratio	7.01
Reynolds number	1.7×10^6
Section shape	NACA 0012
Tapered wing [13]	
Wing span	15 ft.
Root chord	2.14 ft.
Taper ratio	2.5
Mean aerodynamic chord	1.59 ft.
Planform area	22.39 ft^2
Aspect ratio	10
Tip twist angle	−3.90 deg.
Reynolds number	3.5×10^6
Section shape	NACA 4420 (root), NACA 4412 (tip)

Table 3 Computational modeling parameters

Parameter	Value
Terms in sine series expansion m	30
Adaptive quadrature absolute tolerance	10^{-4}
Iteration relative tolerance tol	10^{-3}
Consecutive iterations within tolerance N	5
Fading-memory weighting D	0.05

results. This wing uses a NACA 4420 root section and a NACA 4421 tip section, lofted in-between, and a linear twist distribution. The salient parameters for all three wing designs are listed in Table 2.

The parameters used in the computational model are listed in Table 3. The number of terms in the sine series expansion m is based on the complexity of the wing planform geometry and the level of detail required at the wing tips. The adaptive quadrature absolute tolerance is based on the quadrature algorithm chosen and the size of the terms in the integrands given in Eq. (5) [24]. The iteration convergence parameters tol and N are based on the desired level of confidence in the convergence of the circulation distribution. Finally, the fading-memory weighting D is based on values appearing in the literature on iterative lifting-line techniques [15].

Figures 3 and 4 show the lift and drag coefficient comparisons between the experimental and computational results for the elliptical and crescent wings. In Fig. 3, the experimental lift curves from [20] are plotted alongside the lift curve of the NACA 0012 airfoil and the computational results for the wing using the iterative modified Weissinger's method. Since [20] does not include sectional aerodynamic data, they have been generated with JavaFoil using the NACA standard surface finish and the Eppler standard transition model [25]. The computational results indicate that the elliptical wings follow the same trends as their airfoil with a slight decrease in angle of attack, which is to be expected since the theoretical downwash is constant across the span in the linear regime. Furthermore, the slope of the wing (5.12 rad^{-1}) is less than the airfoil (6.82 rad^{-1}) due to the finite aspect ratio of the wing [26]. These trends weaken at higher angles of attack, as the linear aerodynamic assumptions are no longer valid. Figure 3 also indicates very little difference between the lift curves of the elliptical and crescent wings at low angles of attack, a result supported by the experimental data. The largest discrepancies between the computational and experimental results most likely stem from discrepancies in the sectional data. Had sectional data been available under the same experimental conditions, these would disappear, as is demonstrated with the tapered wing in what follows. The drag polars plotted in Fig. 4 show a good correlation between the calculated and experimental data at low angles of attack, indicating that the induced drag contribution dominates the parasitic drag. Hence, discrepancies in the sectional drag data only manifest at higher angles of attack, as to be expected.

Figures 5 and 6 depicts the experimental and computational data comparisons for the straight tapered wings. The NACA 4420 (root section) and NACA 4412 (tip section) are shown alongside the wing data; these curves are taken from experimental data provided in [13].

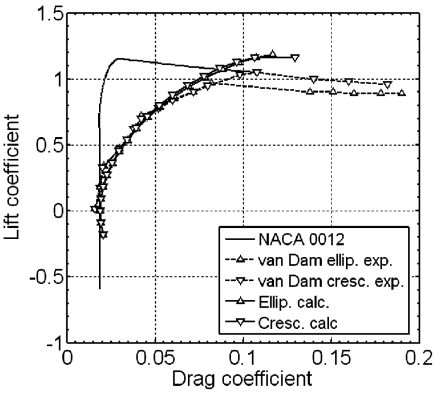

Fig. 4 Drag polars for elliptical and crescent wings. Experimental data are from [20].

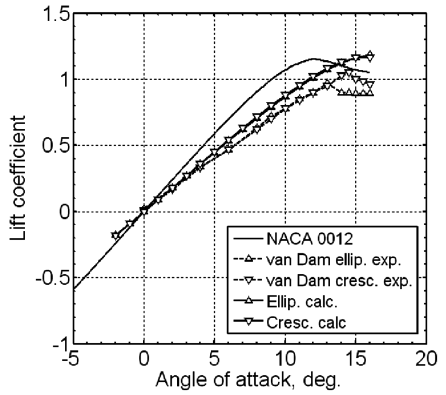

Fig. 3 Lift coefficient vs angle of attack for elliptical and crescent wings. Experimental data are from [20].

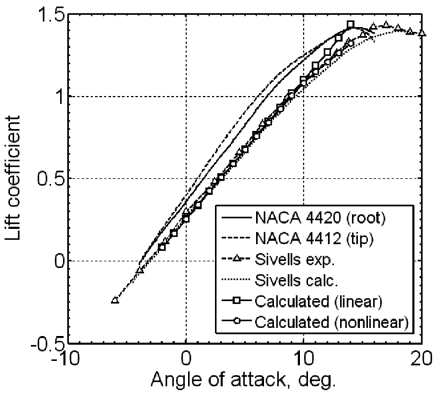

Fig. 5 Lift coefficient vs angle of attack for straight tapered wings. Experimental data are from [13].

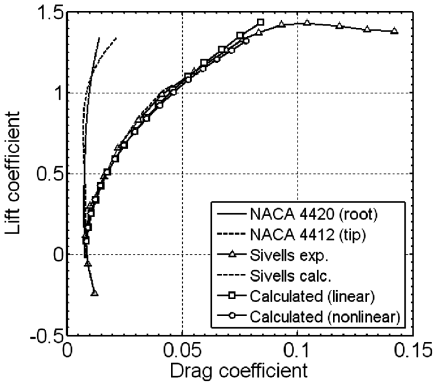

Fig. 6 Drag polars for straight tapered wings. Experimental data are from [13].

For clarity, the intermediate wing sectional data are not shown; however, they generally lie in the span of the two plotted curves. These plots indicate the excellent correspondence between the lift and drag data computed using the present method and the experimental data given in [13]. Furthermore, the present method shows a significant improvement over the nonlinear lifting-line method developed in [13]. As a point of comparison, computed lift and drag coefficients assuming linearized sectional data (i.e., using only the initial stage outlined in Sec. II.A) are shown. As expected, the linearized results are only accurate in the regime wherein the sectional data are linear; in this case, a deviation of at least 5% occurs for $\alpha \geq 11.5$ deg.

IV. Conclusions

An iterative extension of a modified Weissinger's method for curved wings enables viscous flow effects to be introduced into the sectional aerodynamics. This technique can be easily applied to wings whose geometry can be described by a parameterized function and whose sectional aerodynamic data are preestablished and stored in a lookup table. The algorithm derived herein uses the single-step, modified Weissinger's method to establish the initial point of the iterative process that attempts to minimize the difference in the circulation distribution calculated by this method and that given by the sectional aerodynamic data. Three wing shapes are examined using this algorithm and compared with low-speed wind-tunnel results. The results of this comparison indicate that this method corroborates the experimental results well in the attached flow regime and is able to predict the onset of stall over the wings. Also highlighted is the need for accurate sectional data gathered under the same flow conditions as the wing to be analyzed. This method provides a low-order method for aerodynamic calculations, suitable for design or trajectory optimization applications, that nevertheless is able to incorporate nonlinear effects efficiently.

Acknowledgment

The authors would like to thank the anonymous reviewers for their helpful suggestions for improving the validation section.

References

[1] Bowman, J., Sanders, B., and Weisshaar, T., "Evaluating the Impact of Morphing Technologies on Aircraft Performance," AIAA Paper 2002-1631, 2002.

[2] Wickenheiser, A., Garcia, E., and Waszak, M., "Evaluation of Bio-Inspired Morphing Concepts with Regard to Aircraft Dynamics and Performance," *Proceedings of SPIE: The International Society for Optical Engineering*, Vol. 5390, July 2004, pp. 202–211. doi:10.1117/12.540346

[3] Tidwell, Z., Joshi, S., Crossley, W. A., and Ramakrishnan, S., "Comparison of Morphing Wing Strategies Based Upon Aircraft Performance Impacts," AIAA Paper 2004-1722, 2004.

[4] Rodriguez, A. R., "Morphing Aircraft Technology Survey," AIAA Paper 2007-1258, 2007.

[5] Bye, D. R., and McClure, P. D., "Design of a Morphing Vehicle," AIAA Paper 2007-1728, 2007.

[6] Flanagan, J. S., Strutzenberg, R. C., Myers, R. B., and Rodrian, J. E., "Development and Flight Testing of a Morphing Aircraft, the NextGen MFX-1," AIAA Paper 2007-1707, 2007.

[7] Wickenheiser, A., and Garcia, E., "Optimization of Perching Maneuvers Through Vehicle Morphing," *Journal of Guidance, Control, and Dynamics*, Vol. 31, No. 4, 2008, pp. 815–823. doi:10.2514/1.33819

[8] Prandtl, L., and Tietjins, O. G., *Applied Hydro- and Aeromechanics*, McGraw–Hill, New York, 1934; reprint Dover, New York, 1957.

[9] Munk, M. M., "The Minimum Induced Drag of Airfoils," NACA Rept. 121, 1921.

[10] Weissinger, J., "The Lift Distribution of Swept-Back Wings," NACA TM-1120, 1947.

[11] Tani, I., "A Simple Method of Calculating the Induced Velocity of a Monoplane Wing," Tokyo Imperial Univ., Aeronautical Research Inst., Rept. 111, Tokyo, Aug. 1934.

[12] Multhopp, H., "Die Berechnung der Auftriebsverteilung von Traflugein," *Luftfahrtforschung*, Vol. 15, No. 14, April 1938, pp. 153–169.

[13] Sivells, J. C., and Neely, R. H., "Method for Calculating Wing Characteristics by Lifting-Line Theory Using Nonlinear Section Lift Data," NACA TN 1269, April 1947.

[14] Anderson, J. D., Jr., Corda, S., and Van Wie, D. M., "Numerical Lifting Line Theory Applied to Drooped Leading-Edge Wings Below and Above Stall," *Journal of Aircraft*, Vol. 17, No. 12, 1980, pp. 898–904. doi:10.2514/3.44690

[15] Owens, D. B., "Weissinger's Model of the Nonlinear Lifting-Line Method for Aircraft Design," AIAA Paper 98-0597, 1998.

[16] Prössdorf, S., and Tordella, D., "On an Extension of Prandtl's Lifting Line Theory to Curved Wings," *Impact of Computing in Science and Engineering*, Vol. 3, No. 3, 1991, pp. 192–212. doi:10.1016/0899-8248(91)90007-H

[17] Chiocchia, G., Tordella, D., and Prössdorf, S., "The Lifting Line Equation for a Curved Wing in Oscillatory Motion," *Zeitschrift für Angewandte Mathematik und Mechanik*, Vol. 77, No. 4, 1997, pp. 295–315. doi:10.1002/zamm.19970770419

[18] Wickenheiser, A. M., and Garcia, E., "Aerodynamic Modeling of Morphing Wings Using an Extended Lifting-Line Analysis," *Journal of Aircraft*, Vol. 44, No. 1, 2007, pp. 10–16. doi:10.2514/1.18323

[19] Phillips, W. F., and Snyder, D. O., "Modern Adaptation of Prandtl's Classic Lifting-Line Theory," *Journal of Aircraft*, Vol. 37, No. 4, 2000, pp. 662–670. doi:10.2514/2.2649

[20] van Dam, C. P., Vijgen, P. M. H. W., and Holmes, B. J., "Experimental Investigation of the Effect of Crescent Planform on Lift and Drag," *Journal of Aircraft*, Vol. 28, No. 11, 1991, pp. 713–720. doi:10.2514/3.46087

[21] Pistolesi, E., "Considerations Respecting the Mutual Influence of Systems of Airfoils," *Collected Lectures of the 1937 Principal Meeting of the Lilienthal Society*, Berlin, 1937.

[22] DeYoung, J., and Harper, C. W., "Theoretical Symmetric Span Loading at Subsonic Speeds for Wings Having Arbitrary Plan Form," NACA Rept. 921, 1948.

[23] Piszkin S. T., and Levinsky, E. S., "Nonlinear Lifting Line Theory for Predicting Stalling Instabilities on Wings of Moderate Aspect Ratio," General Dynamics Convair, Rept. CASD-NSC-76-001, 1976.

[24] Gander, W., and Gautschi, W., "Adaptive Quadrature—Revisited," *BIT*, Vol. 40, 2000, pp. 84–101. doi:10.1023/A:1022318402393

[25] Eppler, R., and Somers, D., "A Computer Program for the Design and Analysis of Low-Speed Airfoils," NASA TM-80210, 1980.

[26] Katz, J., and Plotkin, A., "Finite Wing: The Lifting Line Model," *Low-Speed Aerodynamics*, 2nd ed., Cambridge University Press, Cambridge, England, U.K., 2001, pp. 173–8.